Combination of Fluorescence-Guided Surgery With Photodynamic Therapy for the Treatment of Cancer

Jun He, MD[1], Leping Yang, MD[1], Wenjun Yi, MD[1], Wentao Fan, MD[1], Yu Wen, MD[1], Xiongying Miao, MD[1], and Li Xiong, MD[1]

Abstract

Specific visualization of body parts is needed during surgery. Fluorescence-guided surgery (FGS) uses a fluorescence contrast agent for in vivo tumor imaging to detect and identify both malignant and normal tissues. There are several advantages and clinical benefits of FGS over other conventional medical imaging modalities, such as its safety, effectiveness, and suitability for real-time imaging in the operating room. Recent advancements in contrast agents and intraoperative fluorescence imaging devices have led to a greater potential for intraoperative fluorescence imaging in clinical applications. Photodynamic therapy (PDT) is an alternative modality to treat tumors, which uses a light-sensitive drug (photosensitizers) and special light to destroy the targeted tissues. In this review, we discuss the fluorescent contrast agents, some newly developed imaging devices, and the successful clinical application of FGS. Additionally, we present the combined strategy of FGS with PDT to further improve the therapeutic effect for patients with cancer. Taken together, this review provides a unique perspective and summarization of FGS.

Introduction

The preoperative detection, localization, and assessment of the tumor demarcation from normal tissues are of great clinical significance for surgeons to evaluate the resectability of malignant tissues. However, in the operating room, the surgeons can predominantly use visual examination and palpation to determine the extent of the tissues to be removed. Palpation or visual examination may be insufficient for a surgeon to confirm and locate all tumor sites via intraoperative detection, particularly for some nonpalpable and invisible occult tumors.[1] Some vital organs, such as the brain, require not only complete removal of the malignant tissues but also maximal preservation of the normal tissues with minimal damage. Although modern intraoperative technologies such as the intraoperative injection of visible dyes and the application of radio-guided occult lesion localization can indeed provide tremendous amounts of information for surgeons during procedures, real-time imaging is urgently required for patients undergoing surgery, considering the changes occurring in their bodies. This demand gave birth to intraoperative visual fluorescence imaging techniques and fluorescence-guided surgery (FGS). This technical procedure includes preoperative or intraoperative administration of

fluorescent agents to the targeted tissues as a preparation, excitation of the fluorescent agents that have accumulated in specific tissues with a laser beam, and monitoring of the fluorescence emission intensity during surgery under a fluorescence microscopy camera.[2] Currently, at least 3 fluorescent contrast agents, including indocyanine green (ICG), 5-aminolevulinic acid (5-ALA), and methylene blue (MB), have been successfully applied in clinical usage for FGS.[3-5] The agents that are used for FGS can also serve as photosensitizers for photodynamic therapy (PDT) and could thus also mediate fluorescence imaging, which is designated as photodynamic diagnosis (PDD).[6]

Fluorescence-guided imaging techniques have clinical advantages and disadvantages compared with the conventional

[1] General Surgery Department, Second Xiangya Hospital, Central South University, Changsha, China

Corresponding Author:
Li Xiong, General Surgery Department, Second Xiangya Hospital, Central South University, Changsha 410011, China.
Email: lixionghn@163.com

imaging modalities. They are much safer and cause less damage in patients due to their nonradioactive labeling properties.[1] Because the near-infrared (NIR) light is invisible to the human eye and because a very dilute fluorescent contrast agent is required, this technology does not alter the appearance of the surgical field. However, the fluorescence imaging can only reach a limited depth in contrast to that of radio-based imaging modalities because visible light can only penetrate micrometer distances and NIR light (700-900 nm) can travel several millimeters in tissues.[1] In contrast, a high signal to background noise ratio provided by the fluorescence signal, especially the NIR light, can lead to a high contrast and resolution of the relatively superficial structures in the surgical scenario. In addition, great advancements have been achieved in the modification of intraoperative fluorescence imaging devices (IFIDs), thus enabling surgeons to simultaneously view the fluorescent and color images.[7-9] Although FGS has exhibited a great potential to improve the intraoperative ability to detect and discriminate tumors from normal tissues, a combined strategy with PDT might be more efficient to eradicate occult and residual tumors. The PDT, which generates a cytotoxic singlet oxygen through interactions between optical light and a photosensitizer in the presence of oxygen, is emerging as a useful and localized treatment for tumors.[10,11] Because many photosensitizers can also be employed as contrast agents, it is highly feasible to harness these photosensitizers as dual-functional agents for clinical applications. However, most free-form photosensitizers lack sufficient solubility and active targeting, which hampers their accomplishment of dual functions in vivo.[12] The recent progression of multifunctional platforms has attracted significant attention, and they are based on nanoparticles and are equipped with active targeted moieties and integrated, but not limited to, fluorescence imaging and PDT.[13,14] It is speculated that the combination of FGS with PDT might be established on multifunctional platforms.

Herein, we discuss the fluorescent contrast agents that are most widely used for FGS, the newly developed IFIDs, and the successful clinical application of FGS for treating tumors and lymph node metastases. We also present the combined strategy of FGS with PDT and the development of multifunctional platforms that might be a promising resolution for this strategy.

Intraoperative Fluorescence Imaging

Current methods for tumor margin detection predominantly involve palpation and visual inspection in the operating room.[1] To obtain precise, specific, and radical resection of cancerous tissues, many preoperative and intraoperative imaging modalities engage in demarcation of malignant margins and metastasis and the preservation of normal tissues. Conventional methodologies, including computed tomography, magnetic resonance imaging (MRI), positron emission tomography (PET), and ultrasound scans, can provide massive amounts of information for surgeons during operations.[15] When these scans are repeatedly conducted and updated throughout surgery, a consecutive visualization of the cancer morphologies

can be obtained. Although these procedures suffer from poor tissue contrast and unsatisfactory spatial resolution, their advantages, such as their real-time and intuitionistic presentation, can dramatically facilitate intraoperative manipulation.[16-18] Additionally, the traditional imaging modalities mentioned above contain several limitations for use in the surgical arena.[19] First, the imaging instrumentations are too cumbersome or dangerous to be positioned in the busy operating room. Although miniaturized and portable devices might be developed, the high magnetic fields from MRI still hinder their wider application. However, the contrast agents for PET are radiolabeled chemicals, such as fludeoxyglucose (^{18}F-FDG) or ^{15}O, ^{11}C, and ^{64}Cu, which can spontaneously convert a proton to a neutron and result in the emission of a positron. Analogically, other radio-based imaging modalities also require the preadministration of radionuclides into the patients, thus leading to significant safety concerns.[19] Furthermore, these aforementioned imaging technologies exhibit no limitations in terms of depth penetration in the body, which cannot offer the desirable contrast and spatial resolution for surgical guidance.[19] Of note, recent endeavors have paved the way for precise surgical navigation with visible and NIR fluorescence optical imaging.

Fluorescence imaging detects the fluorescence signal emitted by a fluorophore that is preintroduced and absorbed into specific cells or tissues and then illuminated by the corresponding incident wave light. The visible light can penetrate tissue on the micrometer scale, whereas NIR light (700-900 nm) can travel through blood and tissue several millimeters, reaching even 1 cm.[1] However, the shortened propagating distance compared with the radioactive rays allows the precise identification of targets beneath the surface. The fluorescent signal with limited penetration ability provides a very detailed image with high spatial and temporal resolution when the signal can be appropriately collected and corrected.[1] Strikingly, the optical imaging based on the NIR window has attracted significant research attention because of the several advantages presented by the NIR spectrum.[20] First, many biological compounds exhibit autofluorescence within the ultraviolet (<400 nm) and visible (400-650 nm) wavelength regions. The heterogeneous signals originating from multiple sources, including the intrinsic biological fluorescence signal and extrinsic contrast agents, makes it too difficult to discriminate the targeted tissues from the normal ones. Second, many endogenous chromophores in normal tissues mainly absorb and scatter visible light other than NIR light. Thus, the attenuation is highly minimized in the NIR region, and NIR fluorescence imaging is inherently safer when applied in patients. Additionally, the scattered light from the excitation source is highly reduced in the NIR region compared with visible light as a function of the principle that the scattering intensity is proportional to the inverse fourth power of the wavelength. These features contribute to an excellent signal to background ratio (SBR) or signal to noise ratio for NIR fluorescence imaging in tissues.[20] Moreover, the development of targeted contrast agents improves SBR even more significantly by enhancing the selective accumulation in targeted tissues and simultaneously

reducing nonspecific bindings. In a nutshell, intraoperative fluorescence imaging, especially those utilizing NIR light, exhibits high contrast, spatial resolution, and safety compared with conventional modalities.

Contrast Agents

The intraoperative fluorescence imaging system requires the in situ excitation of exogenous fluorophores that emit a longer wavelength with improved tissue penetrating ability. To perform the visualization procedure based on the fluorescent signal, 2 fundamental elements should be optimized: the administration of a proper contrast agent and an efficient intraoperative imaging device. There was great enthusiasm for the development of contrast agents with excellent characteristics suited for intraoperative fluorescence imaging. Basically, several crucial parameters should be considered, including a high solubility, extinction coefficient with a large Stokes' shift, quantum yield, and photobleaching threshold.[21,22] Herein, we do not detail the distinct physicochemical and optical properties of the contrast agents that are currently available or still being developed for intraoperative fluorescence imaging. This information can be gained in reference articles.[19,23] Although a variety of contrast agents have been shown to be suitable for fluorescence imaging in vitro and in vivo, only a few agents have been applied to FGS. Notably, almost all of them can also serve as photosensitizers, including ICG, 5-ALA, and MB.[24-26]

Indocyanine green. Indocyanine green, with absorption and emission maxima of 780 nm and 820 nm, respectively,[27] is a classic photosensitizer that can produce toxic chemical species and heat when excited at the proper wavelength. However, its pronounced drawbacks have limited its wider application in PDT, photothermal therapy, and imaging. These drawbacks include a low fluorescence quantum yield, aqueous instability, a short circulation time, and photodegradation, as well as a lack of specificity to tumor tissues.[28] To improve performance in clinical applications, ICG has been encapsulated into a variety of nanoparticles and equipped with targeting moieties or incorporated into multifunctional platforms.[29,30] In the realm of molecular imaging, these strategies significantly promote the tissue signal of interest and simultaneously decrease the background signal. Clinically, the vast majority of surgical techniques performed with ICG are based on the free form.

Indocyanine green is the most widely used contrast agent in surgical navigation and is one of the few NIR contrast agents that is approved by the Food and Drug Administration (FDA) and European Medicines Agency for clinical use.[27] Indocyanine green has a relatively short circulation half-life (150-180 seconds), which limits the total amount of ICG delivered to tumors and ultimately reduces the contrast enhancement.[31] The conventional fluorophores mentioned above such as ICG and 5-ALA are highly susceptible to photobleaching, which leads to significant limitations in the fluence rate.[19] However, ICG can selectively accumulate in or around tumors, and it is thus suitable for the intraoperative imaging of tumor margin and residual. The effectiveness of intraoperative fluorescence imaging guidance with ICG or its modified forms has been validated repeatedly in a variety of preclinical and clinical applications. For example, imaging-guided sentinel lymph node (SLN) mapping based on ICG has been applied in various cancer types, including breast, skin, colorectal, cervical, vulvar, lung, gastric, esophageal, and endometrial cancers.[1] In fact, ICG tends to bind to serum proteins in vivo and to behave as a macromolecule, thereby increasing the hydrodynamic diameter and fluorescence intensity. Thus, this effect would provide a better retention rate for ICG and facilitate the detection of cancerous tissues.[32]

5-Aminolevulinic acid. 5-Aminolevulinic acid is a natural metabolite that is produced via the hemoglobin metabolic pathway.[33] When administered topically or orally, 5-ALA can induce the synthesis and accumulation of a photosensitive and fluorescent molecule called protoporphyrin IX (PpIX) in neoplastic tissues.[34] The selective accumulation of PpIX is mainly correlated with the low expression of 1 enzyme, ferrochelatase, in malignant tissues compared with most normal tissues.[34] The PDT mediated by 5-ALA has gained great interest in the treatment of various tumors, such as brain, lung, esophageal, gastrointestinal, bladder, prostate, head and neck, oral, and skin cancers.[35] Apart from its selectivity per se, nanoparticle-based approaches and active targeting methods can further enhance the selective accumulation of PpIX in cancer tissues.[36,37] The fluorescence signal emitted by PpIX can be detected and used to discriminate cancer tissues from normal tissues. Furthermore, a combined strategy based on 5-ALA can be adopted for theranostic applications.[38]

In the European Union, 5-ALA has been authorized for the fluorescence-guided resection of malignant glioma since 2007.[39] Protoporphyrin IX within malignant tissues can be excited at a wavelength of 405 nm and has an emission peak with approximately half the emitted fluorescence at approximately 635 nm.[40,41] Visual red fluorescence emission combined with a distinct background, such as mucosal tissue exhibiting white color, can provide sufficient contrast for surgical guidance.[42] Because exogenous 5-ALA can conveniently penetrate the blood–brain barrier and travel further into the brain, this agent is highly recognized and extensively applied to the fluorescence visualization of brain tumors. However, it is relatively uncontrollable to modulate the fluorescence signal induced by 5-ALA because they are dramatically influenced by the metabolic activity of tumor cells.[43]

Methylene blue. Methylene blue is a widely known histological dye with a characteristic color caused by the strong absorption band in the 550- to 700-nm region.[26] After decades of endeavors, the basic features of the photodynamic activity of MB have been illuminated, and PDT mediated by MB has also progressed in clinical practice against various tumors.[26] Furthermore, recent advancements in nanoscale materials and active targeting strategies have significantly improved the

therapeutic efficiency and decreased the side effects of PDT with MB.[44]

Methylene blue has been used as a visible (dark blue) dye in surgery for many years.[45] The reflectance images mainly emphasize the highly scattering connective tissues of blood vessels rather than cancer cells.[45] However, dilute MB exhibits an almost undetectable color to the human eye and can serve as a moderate-strength fluorophore that emits at approximately 700 nm.[46-48] Because MB is excreted by the liver and kidneys, it is suitable for visualization of the biliary tract, ureters, and arteries under NIR lighting.[49] In fact, MB can not only function as a perfusion tracer in vivo but it can also facilitate the clear definition of SLNs, tumors, and vital structures through NIR fluorescent imaging.[5,50,51]

Intraoperative Fluorescence Imaging Devices

Appropriate fluorescence contrast agents and IFIDs are the 2 essential elements in procedures for intraoperative FGS. The IFID should be able to capture, recognize, analyze, and send out the fluorescence signal. Practically, these systems often comprise a camera, a light source and excitation module, an optics device for light perception, a computer with analytical software, and a mechanical structure to support the whole system.[52] To reduce the interference of IFID in the conventional operative workflow, imaging systems can also be integrated with preexisting devices in the operating room, such as the optical microscope.[53]

In general, several properties should be included in an ideal IFID in the operating room.[52] First, it should be competent to excite certain fluorescence contrast agents and detect the signal emission from the fluorophores on a macroscopic scale. Second, an IFID would be preferentially equipped with a variety of light sources and various tracers to emit and recognize a wide range of spectra to achieve different surgical purposes. Third, considering the circumstances in the operating room, the device should be portable, adjustable, and amenable to sterilization. Furthermore, the interpretation and presentation of the optic signal should be straightforward and digital, which make it easier to read. Finally, the price of the devices should be reasonable for its further development. We depict the progression of IFID systems for FGS in the following paragraphs, and some advanced and representative devices are illustrated in Figure 1.

Conventional fluorescence imaging systems use dark-field imaging for laparoscopic surgery, resulting in great difficulties in the visualization of nonfluorescent images and significant interruptions of the surgical workflow during the image switching procedure.[7] To overcome these shortcomings, a brightfield/color fluorescence camera of the HyperEye Medical System (Mizuho Co, Tokyo, Japan) has been developed for gastroenterological surgeries.[56] The PINPOINT endoscopic fluorescence imaging system (Novadaq, Mississauga, Ontario, Canada) can overlay color and fluorescent images in a synchronous fashion for integrating normal and fluorescent images.[55] This system can be used in fluorescence imaging of the cystic duct, common bile duct, and gallbladder. The first generation of a surgical imaging system was developed in Beth Israel Deaconess Medical Center, that is, FLARE (fluorescence-assisted resection and exploration), and this device has undergone considerable refinements and modifications over the decades, including a hands-free operation system with more compact optics and an interpretive software.[9] Furthermore, this imaging system has been successfully applied to the first-in-human testing for SLN mapping in breast cancer. This system allows the simultaneous detection and presentation of the color video and NIR fluorescence emission, as well as acquisition of the camera image in real time.[9]

An NIR fluorescence thoracoscope (SPY scope; Novadaq Technologies Inc) has been approved by the FDA and Health Canada for a rigid thoracoscope with a 0-degree endoscopic view. This system can provide both color and NIR fluorescence images simultaneously without distortion of the surgical view.[57] Wada et al developed a minimally invasive SN mapping system that integrated the preoperative transbronchial ICG injection with intraoperative NIR thoracoscopic imaging and optimized multiple factors to determine the fluorescence intensity in porcine lungs.[57] Regarding segmentectomy, Oh et al developed an intraoperative color and fluorescence imaging system (ICFIS) that could visualize the area of interest by merging the fluorescent signals with the anatomical color images.[8] Furthermore, the studies were conducted to validate the image-guided segmentectomy using ICFIS in animal models and to determine the optimal dosage of contrast agent ICG to ensure a safe and efficient fluorescent signal during surgery.

Okusanya et al developed a portable, modular IFID for FGS.[52] This system comprised an NIR charged–coupled device camera, an adjustable filter, an LED light source, and an image presentation system. The system was able to distinguish the NIR signal in tissues with a high SBR in either the laboratory or the clinical setting.

In neurosurgery, a microscope-integrated fluorescent module has been developed that could allow a surgeon to observe the low fluorescence signal from fluorescein without disrupting the workflow of microsurgery under the operating room microscope.[58]

A wearable real-time fluorescence imaging and display system, the fluorescence goggle, was developed at Washington University.[59,60] The fluorescence intensity of tissues can be interpreted and presented directly in the goggle eyepiece, which can be easily worn by a surgeon. Thus, the system can provide a surgeon with a broad range of views that change with the wearer's head movement and gaze direction. The success of this type of system has demonstrated the feasibility of imaging hepatocellular carcinoma (HCC) intraoperatively with high contrast via the transarterial hepatic injection of ICG.[59] Of note, this fluorescence goggle system is simple and cheap, and it has great value for guiding accurate tumor resection.

An important issue that should be considered is the light source in the operating room. The frequently used over-the-bed operating room lights and headlamps could be problematic for intraoperative imaging because they emit white light and
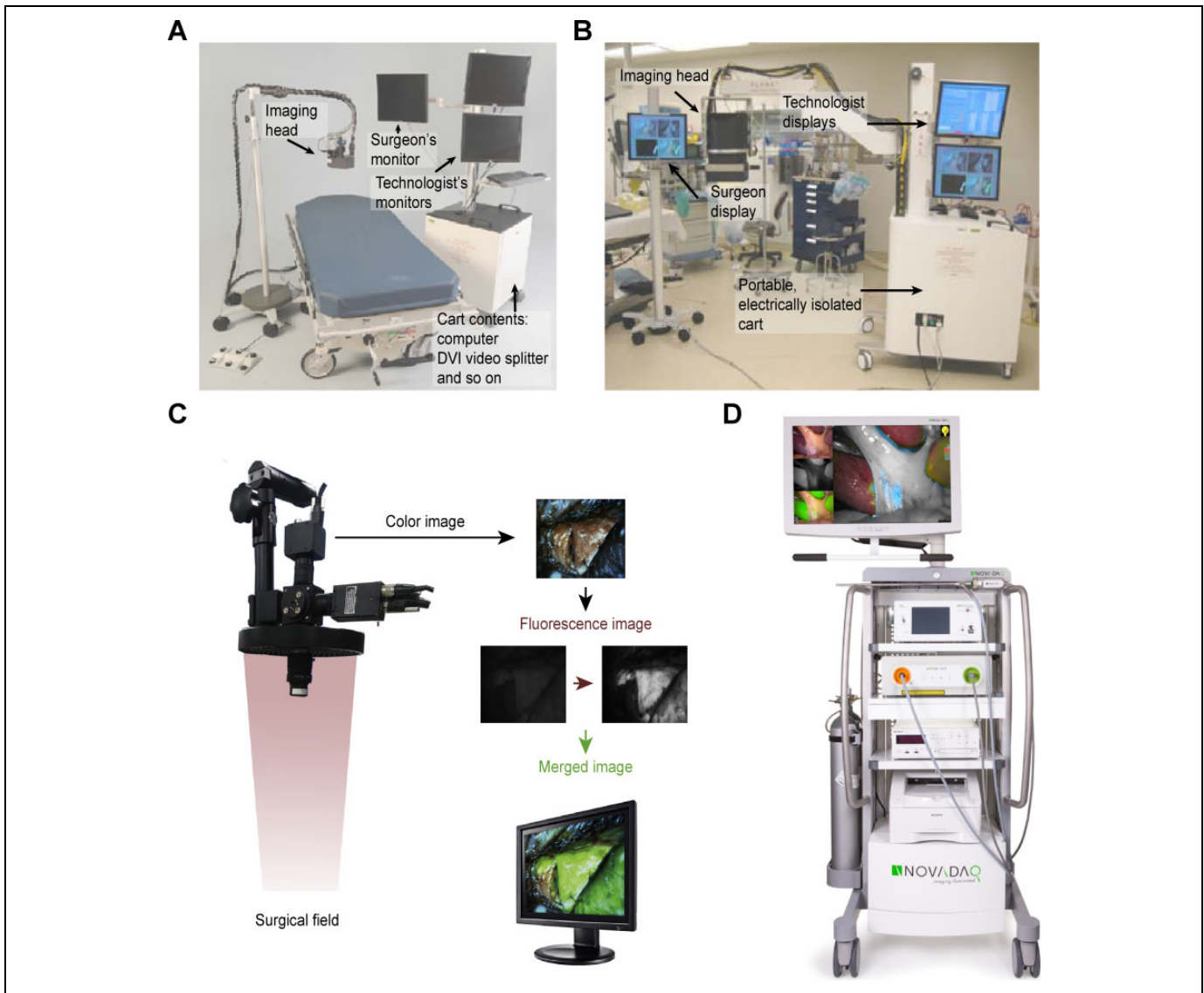
Figure 1. Schematics of several advanced intraoperative fluorescence imaging systems. A, Mini-FLARE (fluorescence-assisted resection and exploration) portable near-infrared fluorescence imaging system.[54] B, FLARE surgical imaging system.[9] C, Intraoperative color and fluorescence imaging system (ICFIS).[8] D, PINPOINT endoscopic fluorescence imaging system.[55]

NIR light, resulting in a false-positive signal.[61] Keating et al developed and tested a novel headlamp system that could filter out the NIR light and provide a clear scenario for intraoperative fluorescence imaging.[62] This system is modified by a standard surgical headlamp with the simple improvement of an additional 2 sequential 25-mm-diameter heat-absorbing glass filters.

Clinical Applications of FGS for Tumors

Sentinel Lymph Node Mapping

The presence of lymph node metastases in patients with tumor is an essential prognostic factor and an important indicator for therapeutic modulation. In a variety of cancers, SLN mapping is currently accepted as a standard of care, such as in breast cancer and cutaneous melanoma.[1] During surgery, identifying metastatic nodes or conducting SLN mapping, along with lymph nodes dissection, is an intractable issue. Clinically, sentinel lymph node biopsy (SLNB) is predominantly performed using 3 modalities, including the injection of radioactive tracer, a visible blue dye (isosulfan blue or patent blue), or both.[63,64] The advantages of visible dye–guided lymph node mapping are its ease of use, cost-effectiveness, and safety, whereas its disadvantages include a lower detection rate compared with radiocolloid, the potential risk of leakage, and halation of the image induced by adaptation of the dyes.[65] Although preoperative lymphoscintigraphy facilitates the intraoperative identification of lymph node with high efficiency, the cost of radiocolloids and the health-care professional equipment, as well as the heavy hardware, hinder its wider application in SLN mapping.

The recent introduction of fluorescence-guided SLN mapping has been extensively examined in various clinical
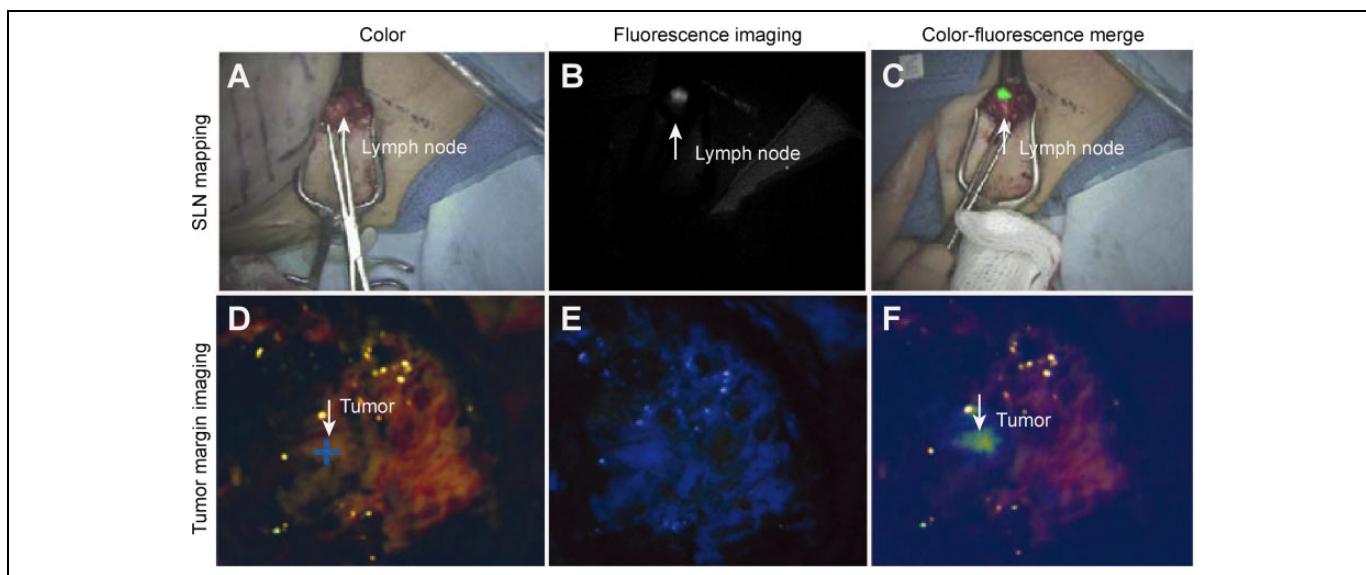
Figure 2. Clinical applications of intraoperative fluorescence imaging. A to C, The present near-infrared (NIR) fluorescent sentinel lymph node mapping in a female patient with breast cancer. A, The color image. B, The NIR fluorescence image. C, The merged pseudocolored image from (A) and (B).[9] D to F, The present fluorescence imaging of the tumor margin during the surgical resection of glioblastoma multiforme. D, Color image. E, Visible fluorescence image. F, Merged pseudocolored image from (D) and (E).[66]

scenarios, including breast cancer, colorectal cancer, vulvar cancer, lung cancer, gastric cancer, melanoma, and esophageal cancer. A representative result is shown in Figure 2A to C.[67,68] The prevailing advantages of SLN mapping using fluorescence imaging include a low concentration of the required contrast agent, no apparent staining of the surgical field compared with visible dyes, and no ionizing radiation, as well as increased spatial and temporal resolution compared with radiotracers.[69] Additionally, fluorescence imaging can provide not only image of SLNs but also a real-time transcutaneous and intraoperative visualization of lymphatic vessels by monitoring the fluorescence signal from the point of the contrast agent administration.[70-72]

The recommended method to record the fluorescence signal is through continuous transcutaneous monitoring or real-time visualization because the entrance timing and endurance of contrast agents in SLNs might be quite variant. Thus, a snapshot of the fluorescence signal may omit valuable information, and the choice of timing is clearly difficult and too experiential. The whole time required for the fluorescence-guided SLN mapping procedure ranged from 8 to 25 minutes and the mean time was 15 minutes in a study of 25 consecutive patients with breast cancer.[73] In the following sections, we list some representative studies that have examined fluorescence-guided SLN in various cancer types.

Large validated studies, including the Axillary Lymphatic Mapping Against Nodal Axillary Clearance trials, showed that SLNB is a safe and reliable method to accurately stage the axillary lymph node in breast cancer.[63] In an initial study, the lymphatic channels draining from the areola to the axilla were immediately imaged, and SLNs could be dissected under fluorescence guidance.[73] A pathological method confirmed the

lymph node metastases identified by the fluorescence signal, with no false-negative cases. In another study, the detection rate was 97.7%, and the sensitivity of metastatic involvement in the SLNs among 43 patients was 94.4%. Furthermore, a low false-negative rate was indicated by only 1 case exhibiting no positive fluorescence signal in SLNs.[70] Compared with the blue dye, the detection rate of SLNB was higher in fluorescence imaging (97.2% vs 81.3%), and the numbers of identified SLNs indicated the advantage of fluorescence-guided SLNB (3.6 vs 2.1).[74] The capacity of NIR fluorescence imaging for SLNs was comparable to that of lymphoscintigraphy in patients with breast cancer.[9] A study showed that a total of 35 SLNs were detected using a radioactive method, equivalent to the results obtained by NIR fluorescence mapping.[54]

In colon cancer, conventional methods for SLNB are based on radiocolloid, blue dye, or a combination of both, and the detection rate ranges from 81% to 98%, with a sensitivity up to 90%.[75-77] Fluorescence-guided SLN imaging possesses several advantages over conventional modalities, as presented in the upper section. In pigs, SLNs can be identified with an accuracy of 100% under both in vivo and ex vivo conditions.[78] In the same study, this method led to the successful detection of SLNs in all 24 consecutive patients, and the average number of SLNs was 3.0. Analogously, another report showed that ICG fluorescence imaging could identify 1.7 SLNs, on average, with a detection rate of 96% and a sensitivity of 82%.[75] Intriguingly, this method could also be used to detect tumoral lymph nodes in colorectal cancer, such as retroperitoneal and mesocolic lymph node metastases.[79]

Regarding gastric cancer, a study showed that the visualization of lymphatic vessels draining from the primary gastric tumor toward the lymph nodes could be easily achieved under

a laparoscopic ICG fluorescence imaging system among all patients with clinical T1 gastric cancer.[80] In another study, 31 patients were tested for NIR imaging-ICG guidance during robotic gastrectomy.[81] A mean lymph node retrieval of 29 was achieved in adenocarcinoma resections and 5 in wedge resections. Thus, fluorescence imaging is a useful method for visualizing lymph nodes during minimal access surgeries.

A minimally invasive laparoscopic approach combined with NIR imaging–guided SLN mapping is also used in cervical cancer. A recent study performed simple or radical laparoscopic hysterectomy along with SLN mapping by NIR imaging on 49 patients with clinical stage I cervical cancer or stage I endometrial cancer.[68] The results revealed a detection rate of 100%, and the sensitivity and negative predictive value of SLN detection were both 100%. Another study indicated that fluorescence-guided technology could be capable of the simultaneous mapping of pan lymph nodes and SLNs in the same subject. This dual-channel intraoperative imaging system could identify and resect all pan lymph nodes and SLNs in patients with cervical cancer.[7]

Tumor Imaging

Intraoperative tumor detection can significantly improve the integrity and accuracy of malignant tissue resection.[82] However, the current modalities for intraoperative tumor margin assessment, such as frozen section techniques, intraoperative ultrasound, imprint cytology, and 2-view specimen mammography, do not fully meet the clinical expectations.[83] These laborious and time-consuming modalities also fail to provide continuous and real-time monitoring during operations.[83] Fluorescence-guided imaging is a promising alternative to provide a high degree of sensitivity and specificity for tumor margin detection and thus perfectly meet the clinical demand. However targeting strategies, such as the utilization of antibodies that can specifically recognize cancer cells or contrast agents that can be activated by tumor-specific enzymes, have been extensively studied.[84,85] To date, none of the active targeted fluorescent contrast agents have been completely approved for clinical applications.

Breast cancer. A research group evaluated the feasibility of intraoperative NIR fluorescence imaging in a simulated clinical environment as an investigation for future NIR fluorescence–guided breast-conserving surgery.[27] In their practice, a gel-based breast phantom that mimics the optical characteristics of breast tissues was used as a model and mixed with tumor-like fluorescent inclusions. Based on this system, a clear change in the signal strength of the fluorescence image occurred during the surgical simulation procedure, which might assist surgeons in carefully advancing the margins.[27] Another research group used ICG intraoperative imaging to detect murine tumors before and after resection, and this imaging procedure demonstrated no significant adverse events.[83] Similarly, it is possible for intraoperative fluorescence imaging to identify almost all patient breast tumors, including

nonpalpable ones (refer to PMID 27756411). Intraoperative NIR fluorescence imaging could also be used to detect the tumor residual in patients after standard surgery.[83] Furthermore, self-assembled ICG nanoparticles functionalized by hyaluronic acid were introduced into FGS.[16] This configuration exhibited significant improvements in specificity for tumor margin imaging and provided higher contrast optical images compared to free-form ICG for surgical removal. More recently, a hybrid tracer with both radioactivity and fluorescence was developed for the combined pre- and intraoperative localization of nonpalpable lesions in breast cancer.[86] Deep tumors in critical locations could be detected by the acoustic signal derived from the gamma ray detection probe, while the targeted lesions could be visualized in a real-time optical image by the ICG fluorescence signal. After excision, the residual lesions could be found based on the anatomical situation visualized by radio guidance combined with visual information.[86]

Liver cancer. The ICG fluorescence imaging has been effectively used to identify microscopically confirmed HCC and liver metastases and provide an intraoperative visualization of the liver segment. The initial study showed that well-differentiated HCCs exhibited regular and highly fluorescent lesions, whereas poorly differentiated HCCs and liver metastases exhibited rim fluorescent-type lesions in tissues.[87,88] This fluorescence imaging modality could delineate any lesions with a limited penetration depth and enable the highly sensitive identification of small liver cancers on surgical specimens. A preclinical study conducted in dogs showed that the sensitivity and the positive predictive value of ICG fluorescence imaging for HCC were 71.4% and 90.0%, respectively.[89] Another study suggested that ICG fluorescence imaging could be applied to detect the extrahepatic metastases of HCC by intravenous injection of the contrast agent.[90] The preclinical data showed that the positive predictive value of intraoperative ICG fluorescent imaging and ICG fluorescent imaging of the patient tissue specimen was both 100%, and the sensitivities were 92% and 96%, respectively. In a systematic study, all liver tumors could be detected by ICG fluorescence imaging.[91] Nevertheless, the overall rate of diagnostic accuracy by ICG fluorescence imaging was lower than that of intraoperative ultrasonography, which is an essential tool for determining the liver tumor location. This discrimination resulted from the different rates of fluorescence of various tumors and the tumor depth as well as the limited size of small tumors.[91]

Meanwhile, a recent study showed that ICG fluorescence imaging for HCC might provide an influential false-negative rate.[59] The tumors in 3 of the 5 considered patients did not exhibit higher fluorescence than the nontumor liver tissue; thus, the fluorescence contrast could not be applied in hepatic surgical resection. Consequently, there is a demand for development of a more tumor-selective molecular probe. A group synthesized arginine–glycine–aspartic acid (RGD)-conjugated ICG mesoporous silica nanoparticles as an intraoperative fluorescent probe and used the probe to test selectivity.[92] The results showed that this novel probe led a significantly enhanced

optical signal in hepatic tumor lesions, provided remarkable optical contrast at the liver tumor margin, and displayed a high potential for the detection of residual microtumors.

Brain cancer. The FGS has attracted great attention globally for the treatment of malignant brain tumors, and most studies have focused on the use of 5-ALA as a fluorescent contrast agent.[6,93,94] A variety of reports have demonstrated that this technique possesses a very high sensitivity and specificity for malignant glioma tissue by 5-ALA guidance because these values were often close to or over 90% (refer to PMID 25946082). A representative result is shown in Figure 2D to F.[33] However, diverse fluorescence patterns can be observed in malignant brain cancers; solid red fluorescence is found in the bulk of malignant glioma tumors, whereas pink fluorescence is mainly exhibited at the tumor margin where cancer cells infiltrate the normal brain.[95-97] The visible fluorescence emitted by tumor tissues could be valuable for predicting the tumor aggressiveness because biopsies from strongly fluorescing tissues predominantly contain high-density, highly proliferating tumors and biopsies from weakly fluorescing tissues mainly contain infiltrating tumors.[98] In a recent study, the ALA intensity was considered a strong predictor of the degree of tumor cellularity in most areas of fluorescence.[99] Because ex vivo quantitative measurements of the PpIX concentration in tissues are more sensitive for identifying malignancy in both low- and high-grade tumors than the intraoperative fluorescence imaging, an improved fluorescence detection technology is needed to achieve improved sensitivity and differentiation of tumors.[100]

Combination strategies have been applied to precisely define the tumor margins. A variety of surgical adjuncts, such as cortical and subcortical mapping, motor-evoked potential monitoring, speech monitoring in awake settings, and early second surgeries for tumor remnants, as well as 5-ALA fluorescence imaging, might contribute to the maximization of tumor resection with an acceptable postoperative deficit.[101] However, multiple studies have shown a histological difference in intraoperative solid tumor depiction using 5-ALA fluorescence imaging and gadolinium-diethylenetriamine pentaacetic acid–enhanced MRI, especially for lesions >9 cm^3 because 5-ALA fluorescing tissues significantly exceed those of MRI-enhanced tissues such as lesion numbers in terms of contrast intensity.[102] The combination of 5-ALA with MRI resulted in a significantly increased extent of resection, but it did not lead to an increase in complications or neurological deficits.[102] Furthermore, intraoperative MRI-guided resection might be a powerful tool to treat 5-ALA-negative gliomas, and 5-ALA showed great potential for high-grade gliomas.[103] Additionally, 5-ALA fluorescence and PET image are distinct index markers for cytoreduction surgery for gliomas because 5-ALA-induced fluorescence and ^{11}C-methionine uptake are independent indices of the tumor cell density.[104]

The modified contrast agent was also developed and applied to visible intraoperative delineation of brain tumors. Another group designed a tumor-targeted dye loaded on nanoparticles and evaluated the in vitro properties.[105] The incubation of glioma cells with dye-loaded NPs could lead to visible, quantifiable cell tagging in a dose- and time-dependent manner. The targeted moiety relied on a peptide, F3, which binds to the tumor cell surface receptor nucleolin. Molecular targeted imaging can further improve the precision of tumor resection with intraoperative fluorescence guidance.

The Combination of FGS With PDT

In the above-described sections, we systematically discuss the primary theoretics and clinical applications of FGS with photosensitizers. The fluorescence signal emitted by photosensitizers provides significant advantages for the intraoperative discrimination of malignant tissues from peripheral normal tissues. In fact, these contrast agents and their modified forms are dual-functional platforms; fluorescence attributes contribute to fluorescence imaging, and PDT utilizes the attributes of photoactivity. Consistent with decades of practice, PDT has been demonstrated to be an efficient modality for various cancers. For example, PDT can induce direct killing and immunological effects on breast cancer (refer to PMID 27833041). The PDT has been also conducted for treatment of primary and metastasizing liver cancer (refer to PMID 12743863; 23377406). In many scenarios, surgical resection remains the only curative modality, and PDT and other therapies such as chemotherapy and radiotherapy have a secondary or an adjunct position. After an extensive interrogation of FGS with photosensitizers, 1 question arises concerning whether a combined strategy integrating FGS with PDT would be an alternative to eradicate cancer cells and improve the prognosis. This question is derived from the observation that FGS cannot guarantee 100% removal of all tumors because tiny invasive tumors or tumors with marginal fluorescence emission might be present.

The combined strategy can be conducted in different procedures: neoadjuvant PDT can efficiently destroy malignant tissues, thereby enhancing resectability or reducing the required resection extent[106]; intraoperative PDT denotes the irradiation of the resection cavity with a proper wavelength during or after surgery[107]; and postoperative PDT is conducted after suture of the incision.[108] The clinical data suggested that a combined strategy could more beneficial to patients with cancer than surgery alone. Neoadjuvant PDT along with chemotherapy has been shown to be effective and safe to facilitate the conversion of surgical candidates in locally advanced non-small cell lung cancer.[106] Intraoperative PDT for primary and recurrent gliomas can, in general, result in an increase in the median survival of patients.[109] Another study showed that the 12-month overall survival rate and 6-month progression-free survival rate were both 100% among newly diagnosed gliomas.[107] Postoperative PDT exhibited great potential to achieve locoregional tumor control or even eradicate residual tumors, which were often the origin of recurrence. In a prospective randomized controlled trial, PDT with ALA and Photofrin significantly improved the eradication of residual tumors and survival rate in patients with glioblastoma multiforme after FGS.[110] In summary, PDT could

be an efficient adjuvant modality and assist surgical resection in eradicating cancer cells.

Because the photosensitizers listed herein could also serve as contrast agents for FGS, the administration of solely 1 agent could accomplish the administration of 2 therapies, that is, FGS and PDT. It would be more economical and simplify the therapeutic procedures than the separated administration of 1 contrast agent for FGS and 1 photosensitizer for PDT. Additionally, consecutively taking advantage of 1 photosensitizer could help reduce the adverse events not only in the severity but also in quantity associated with photosensitive contrast agents such as skin phototoxicity. In an experimental study, combined therapy utilizing ALA as a contrast agent and photosensitizer significantly prolonged the survival of tumor-bearing rabbits compared with the group treated with FGS alone.[111] This regimen might kill the peripheral tumor residual and would clearly delay potential recurrence. In the clinical setting, the combination of PDT with the surgical cavity might be a safe technique that ultimately completes the destruction of tumor cells.[112] Of note, the recent progression in multifunctional platforms has enabled, but has not been limited to, the use of FGS and PDT as 1 agent.

Multifunctional Platforms That Are Suitable for the Combination of FGS With PDT

Although a variety of photosensitizers exhibit excellent photochemical and photophysical properties in vitro for fluorescence imaging and PDT, only a small fraction of them has been incorporated into clinical applications. The dissatisfactory solubility and poor selectivity of photosensitizers are the 2 dominating limitations. A longstanding interest in this research is to develop nanoscale carriers for photosensitizers that would increase their aqueous solubility and enhance cellular internalization.[113] To increase the selective accumulation of photosensitizers in cancer cells, both passive and active targeting strategies have been involved in recent endeavors. Thus, we present some potential photosensitizers that have not been applied in FGS but exhibit sufficient fluorescence properties. Additionally, targeting strategies are discussed in the combination of FGS with PDT.

Potential Photosensitizers

Chlorine e6 (Ce6) has been demonstrated to be an effective alternative for fluorescence imaging and PDT. It exhibits highly effective NIR light–induced in vivo phototoxicity in cancer cells in mice when absorbed in upconversion nanoparticles.[114] Based on confocal laser scanning microscopy imaging, strong fluorescence was detected inside cancer cells. Another study indicated that Ce6-conjugated polymers could employ dual-modal imaging (MRI and fluorescence imaging) and combined photothermal and PDT.[115] This multifunctional platform exhibited a clearly enhanced inhibitory effect on tumor growth in vitro and in vivo.

Given the strong absorption within the NIR window, phthalocyanine (Pc) has also demonstrated significant potential as a theranostic agent. The Pc-loaded graphene nanoplatform was found to produce efficient fluorescence emission for fluorescence imaging and reactive oxygen species for the destruction of ovarian cancer cells.[116] Additionally, the novel design of highly biocompatible carbon nanodots loaded with zinc Pc could achieve simultaneous fluorescence imaging and PDT in HeLa cells and animal models.[113]

Photochlor, or 2-[1-hexyloxyethyl]-2-devinyl pyropheophorbide-α, a hydrophobic photosensitizer with a peak absorbance at 665 nm, has demonstrated excellent safety and efficacy for the treatment of various cancer types.[117] Fluorescence imaging revealed the tumor selectivity with an approximately 2- to 3-fold differential between tumor and adjacent normal tissues. The incorporation of 2-[1-hexyloxyethyl]-2-devinyl pyropheophorbide-α into Au nanocages significantly improved the efficacy of PDT and showed no toxicity in mice.[118]

Apart from the classic photosensitizers mentioned above, a variety of new photosensitizers are emerging, and the majority of them might also exhibit fluorescence property. One porphyrin derivative, NMM, also named N-methyl mesoporphyrin IX, showed significantly increased fluorescence intensity upon binding to gold nanoparticles.[119] Further, irradiating the conjugate with white light could induce the efficient production of reactive oxygen species for PDT. Another group also designed and tested novel dyad compounds based on porphyrin for their spectral properties.[120] The results suggested promising optical properties and exhibited high light-induced cytotoxicity in vitro. A complete list of photosensitizers that exhibit potential and sufficient value for fluorescence imaging is not present herein.

Improved Targeting

To improve the selective accumulation of photosensitizers and thereby accomplish targeted fluorescence imaging and phototoxicity in cancer cells, targeting strategies should be performed. In general, 3 strategies have been employed to assist in targeting cancer cells and providing enhanced optical contrast between malignant and normal tissues. The first strategy is passive enrichment for cancer, which implies that macromolecular agents, such as nanoparticles, preferentially accumulate in cancers via the effect of enhanced permeability and retention. Second, the development of activatable multifunctional agents with the capacity to respond to a given stimulus is dramatically increasing.[121] Exogenous stimuli (such as the applied magnetic/electrical field, ultrasound, and light) and endogenous stimuli (such as the temperature, pH, and enzymatic activity) could both be utilized and developed to control the activation of multifunctional agents.[122-125] Additionally, an enhanced selectivity and specificity for malignant cells can be achieved through the use of targeted moieties that are able to recognize the specific receptors or ligands distributed on the surface or inside cells.

The passive strategy incorporating the fabrication of nanoscale agents for the delivery of photosensitizers to cancerous

tissues has been extensively reviewed, and it is thus not presented in this article. Nevertheless, we emphasize the active strategies applied to develop multifunctional platforms with clinical potential for combining FGS with PDT.

Activatable nanoparticles can selectively deliver the encapsulated agents to cancer cells. The stable, long-circulating nanoparticles under normal physiological conditions exhibit altered properties in response to some distinct stimuli that are present in malignant tissues. The mildly acidic pH is one of the most widely used features of the cancer microenvironment for the design of activatable nanoparticles.[126] Recently, novel charge-switching nanoparticles were developed. Under slightly acidic conditions, this material will be positively charged, thereby facilitating the interaction with negatively charged cell membranes to enhance the cellular uptake of nanoparticles.[114] Furthermore, pH-responsive nanoparticles incorporating Ce6 exhibited remarkably enhanced tumor-homing abilities and promising applications in cancer theranostics. However, enzymes that are overexpressed in tumor cells can also be utilized for the development of activatable nanoparticles. For example, matrix metalloprotease-2 in cancer cells can activate some fluorescence imaging peptides that are capped on the nanoplatform.[127] Similarly, a smart dual-targeted theranostic agent could become highly fluorescent and phototoxic only when its linker is broken by tumor -associated lysosomal enzyme cathepsin B after internalization into folate receptor–positive cancer cells.[128]

The receptors or ligands that are distinctly or significantly upregulated in cancer cells can direct the selective accumulation of multifunctional agents in malignant tissues. One frequently mentioned ligand is RGD peptide, which can link the integrin $\alpha v\beta 3$ receptor that is overexpressed in many tumor types. A research group synthesized RGD-conjugated highly loaded ICG nanoparticles as a fluorescent probe, which showed great potential for FGS in liver tumor resection.[92] Another group fabricated a multimodal agent by conjugating nanoparticles to (i) temoporfin as a photosensitizer, (ii) the RGD peptide for improved tumor targeting, and (iii) a fluorescent dye molecule for improved contrast.[13] This agent exhibited a high PDT therapeutic efficacy and excellent suitability for in vivo fluorescence imaging. Folic acid (FA) can mediate the endocytosis of folate conjugates by binding to the folate receptor, which is upregulated in many human cancers, such as malignancies of the ovary, lung, brain, and breast.[129] Wang et al reported a nanoparticle that incorporates a fluorescence imaging agent and a photosensitizer functionalized by FA to gain targeting capacity.[130] This multimodal technique exhibited enhanced delivery of photosensitizers and fluorescent dyes to cancer cells and thereby greater potential of theranostic applications. Recently, a novel design of highly biocompatible, fluorescent, FA-functionalized carbon nanodots was developed that showed increased fluorescence efficiency and good cytotoxic effects in vitro and in animal models.[113] More recently, FA-coupled nanoprobe loading with the photosensitizer of Ce6 was designed.[131] The systematic in vitro and in vivo experiments demonstrated that this was a promising multifunctional

theranostic agent with specificity, efficacy, and safety. The aptamer is another interesting molecule, which could specifically bind to the target nucleolin receptor overexpressed on cancer cells.[132] Ai et al reported the synthesis and application of 1 gold nanoparticle modified with an aptamer and conjugated to a photosensitizer.[119] The results supported its efficiency for both targeted cell imaging and PDT. Of note, a variety of other molecules, such as anti-human epidermal growth factor receptor 2 antibody, cholecystokinin-2 receptor, and carbonic anhydrase IX, to name just a few, have been conjugated to nanoparticles, and these advancements might also be applied to multifunctional platforms.[133-136]

Concluding Remarks

Fluorescence imaging techniques have exhibited great potential for improving the accuracy in surgical section and eradicating malignant tissues while preserving normal tissues as much as possible by visualizing tissue demarcations in real time. The fluorescent contrast agents can be administered in either systematic or topical fashion in light of the different purposes, tissue characteristics, features of the fluorescent agents, and instrumental conditions. Currently, the contrast agents that are widely used in intraoperative imaging include ICG, 5-ALA, and MB. These agents are more intensively used as photosensitizers for PDT because of their optical characteristics. Thus, the fluorescence imaging method presented in this review can also be designated and used in PDD. Intraoperative imaging techniques require a synchronous interplay among contrast agents, tumor biology, imaging systems, and image analysis algorithms. The advancement of contrast agents represents specific tumor-targeted molecular imaging by the addition of targeted moieties to contrast agents such as peptides, receptors, and other specific elements that can be recognized and internalized by tumor cells. The recently developed imaging systems merge fluorescent signals with the anatomical color images to simultaneously visualize the normal color and fluorescent images without disrupting the surgical workflow. Extensive clinical applications have been implemented to map SLNs, demarcate the malignant tissues from benign tissues, and protect normal tissues from accidental injury during surgery.

Nevertheless, surgery guided by intraoperative fluorescence imaging is not able to remove every tiny tumor in all clinical scenarios. The FGS combined with PDT might be an alternative strategy based on evidence indicating the benefits of adjunct PDT or neoadjunct PDT for patients with cancer. Furthermore, this combined strategy can be established on one platform incorporating fluorescent and photoactive agents. Considering the clinical condition, it might not be available to accomplish the 2 missions of the free forms of photosensitizers. The recent development of multifunctional platforms shows great potential for the integration of FGS with PDT. These platforms might also resolve several limitations that continue to hamper the wider usage and application of intraoperative fluorescence imaging and PDT. Due to the relatively low depth of tissue penetration of the light during optical

imaging, it currently cannot be used to depict deep tissues or requires combined strategy with other modalities such as radioscintigraphy and ultrasonography. In fact, many multifunctional platforms allow various imaging modalities and therapies to be combined into 1 agent. Moreover, another disadvantage is that the vast majority of contrast agents fail to actively target the tumor cells, resulting in a great insufficiency of the targeted imaging and targeted surgery. Targeted moieties can be equipped on multifunctional platforms for selective accumulation in cancer cells.

Albeit it is beneficial of this combination strategy for tumor elimination, more preclinical and clinical trials are needed to further demonstrate this view. Practically, the procedures should be reasonably simplified and orchestrated, because the addition of PDT to surgery guided by fluorescence imparts complexity to the whole protocol. With the unremitting optimization of preclinical research and the continuous improvements in clinical trials, we believe that image-guided surgery and the combination of PDT will become widely used in clinical applications.

References

1. Vahrmeijer AL, Hutteman M, van der Vorst JR, van de Velde CJH, Frangioni JV. Image-guided cancer surgery using near-infrared fluorescence. *Nat Rev Clin Oncol*. 2013;10(9):507–518.

2. Zaidi N, Bucak E, Okoh A, Yazici P, Yigitbas H, Berber E. The utility of indocyanine green near infrared fluorescent imaging in the identification of parathyroid glands during surgery for primary hyperparathyroidism. *J Surg Oncol*. 2016;113(7):771–774.

3. Crane LM, Themelis G, Arts HJ, et al. Intraoperative near-infrared fluorescence imaging for sentinel lymph node detection in vulvar cancer: first clinical results. *Gynecol Oncol*. 2011; 120(2):291–295.

4. Della PA, Ciccarino P, Lombardi G, Rolma G, Cecchin D, Rossetto M. 5-Aminolevulinic acid fluorescence in high grade glioma surgery: surgical outcome, intraoperative findings, and fluorescence patterns. *Int J Clin Med*. 2014;2014(3):232561.

5. Tummers QR, Verbeek FP, Schaafsma BE, et al. Real-time intraoperative detection of breast cancer using near-infrared fluorescence imaging and methylene blue. *Eur J Surg Oncol*. 2014;40(7):850–858.

6. Yamamoto T, Ishikawa E, Miki S, et al. Photodynamic diagnosis using 5-aminolevulinic acid in 41 biopsies for primary central nervous system lymphoma. *Photochem Photobiol*. 2015;91(6): 1452–1457.

7. Tsutsui N, Yoshida M, Kitajima M, Suzuki Y. Laparoscopic cholecystectomy using the PINPOINT endoscopic fluorescence imaging system with intraoperative fluorescent imaging: a case report. *Int J Surg Case Rep*. 2016;21:129–132.

8. Oh Y, Quan YH, Kim M, Kim BM, Kim HK. Intraoperative fluorescence image-guided pulmonary segmentectomy. *J Surg Res*. 2015;199(2):287–293.

9. Troyan SL, Kianzad V, Gibbsstrauss SL, et al. The FLARE™ intraoperative near-infrared fluorescence imaging system: a first-in-human clinical trial in breast cancer sentinel lymph node mapping. *Ann Surg Oncol*. 2009;16(10):2943–2952.

10. Muhanna N, Cui L, Chan H, et al. Multimodal image-guided surgical and photodynamic interventions in head and neck cancer: from primary tumor to metastatic drainage. *Clin Cancer Res*. 2016;22(4):961–970.

11. Jin CS, Cui L, Wang F, Chen J, Zheng G. Targeting-triggered porphysome nanostructure disruption for activatable photodynamic therapy. *Adv Healthc Mater*. 2015;3(8):1240–1249.

12. Bechet D, Couleaud P, Frochot C, Viriot ML, Guillemin F, Barberiheyob M. Nanoparticles as vehicles for delivery of photodynamic therapy agents. *Trends Biotechnol*. 2008;26(11): 612–621.

13. Haedicke K, Kozlova D, Gräfe S, Teichgräber U, Epple M, Hilger I. Multifunctional calcium phosphate nanoparticles for combining near-infrared fluorescence imaging and photodynamic therapy. *Acta Biomater*. 2015;14:197–207.

14. Wang Y, Wang H, Liu D, Song S, Wang X, Zhang H. Graphene oxide covalently grafted upconversion nanoparticles for combined NIR mediated imaging and photothermal/photodynamic cancer therapy. *Biomaterials*. 2013;34(31):7715–7724.

15. Elliott JT, Dsouza AV, Davis SC, et al. Review of fluorescence guided surgery visualization and overlay techniques. *Biomed Opt Express*. 2015;6(10):3765–3782.

16. Hill TK, Abdulahad A, Kelkar SS, et al. Indocyanine green-loaded nanoparticles for image-guided tumor surgery. *Bioconjug Chem*. 2015;26(2):294–303.

17. Lovrics PJ, Cornacchi SD, Vora R, Goldsmith CH, Kahnamoui K. Systematic review of radioguided surgery for non-palpable breast cancer. *Eur J Surg Oncol*. 2011;37(5):388–397.

18. Im VDP, Hobbelink M, Ma VDB, Mali WP, Borel Rinkes IH, Van HR. 'Radioguided occult lesion localisation' (ROLL) for non-palpable breast lesions: a review of the relevant literature. *Eur J Surg Oncol*. 2008;34(1):1–5.

19. Owens EA, Lee S, Choi J, Henary M, Choi HS. NIR fluorescent small molecules for intraoperative imaging. *Wiley Interdiscip Rev Nanomed Nanobiotechnol*. 2015;7(6):828–838.

20. Frangioni JV. In vivo near-infrared fluorescence imaging. *Curr Opin Chem Biol*. 2003;7(5):626–634.

21. Choi HS, Frangioni JV. Nanoparticles for biomedical imaging: fundamentals of clinical translation. *Mol Imaging*. 2010;9(6): 291–310.

22. Choi HS, Liu W, Liu F, et al. Design considerations for tumour-targeted nanoparticles. *Nat Nanotechnol*. 2010;5(1):42–47.

23. Bu L, Shen B, Cheng Z. Fluorescent imaging of cancerous tissues for targeted surgery. *Adv Drug Deliv Rev*. 2014;76:21–38.

24. Corlu A, Choe R, Durduran T, et al. Three-dimensional in vivo fluorescence diffuse optical tomography of breast cancer in humans. *Opt Express*. 2007;15(11):6696–6716.

25. Peng Q, Berg K, Moan J, Kongshaug M, Nesland JM. 5-Aminolevulinic acid-based photodynamic therapy: principles and experimental research. *Photochem Photobiol*. 1997;65(2): 235–251.

26. Tardivo JP, Del GA, de Oliveira CS, et al. Methylene blue in photodynamic therapy: from basic mechanisms to clinical applications. *Photodiagnosis Photodyn Ther*. 2005;2(3): 175–191.

27. Pleijhuis RG, Langhout GC, Helfrich W, et al. Near-infrared fluorescence (NIRF) imaging in breast-conserving surgery: assessing intraoperative techniques in tissue-simulating breast phantoms. *Eur J Surg Oncol*. 2011;37(1):32–39.

28. Sheng Z, Hu D, Xue M, He M, Gong P, Cai L. Indocyanine green nanoparticles for theranostic applications. *Nano-Micro Letters*. 2013;5(3):145–150.

29. Yuan A, Wu J, Tang X, Zhao L, Xu F, Hu Y. Application of near-infrared dyes for tumor imaging, photothermal, and photodynamic therapies. *J Pharm Sci*. 2013;102(1):6–28.

30. Liu B, Li C, Xing B, Yang P, Lin J. Multifunctional UCNPs@PDA-ICG nanocomposites for upconversion imaging and combined photothermal/photodynamic therapy with enhanced antitumor efficacy. *J Mater Chem B Mater Biol Med*. 2016;4:4884–4894.

31. Saxena V, Sadoqi M, Shao J. Polymeric nanoparticulate delivery system for Indocyanine green: biodistribution in healthy mice. *Int J Pharm*. 2006;308(1-2):200–204.

32. Ohnishi S, Lomnes SJ, Laurence RG, Gogbashian A, Mariani G, Frangioni JV. Organic alternatives to quantum dots for intraoperative near-infrared fluorescent sentinel lymph node mapping. *Mol Imaging*. 2005;4(3):172–181.

33. Hadjipanayis CG, Widhalm G, Stummer W. What is the surgical benefit of utilizing 5-aminolevulinic acid for fluorescence-guided surgery of malignant gliomas? *Neurosurgery*. 2015;77(5): 663–673.

34. Collaud S, Juzeniene A, Moan J, Lange N. On the selectivity of 5-aminolevulinic acid-induced protoporphyrin IX formation. *Curr Med Chem Anticancer Agents*. 2004;4(3):301–316.

35. Zhang X, Liu T, Zhihong LI, Zhang X. Progress of photodynamic therapy applications in the treatment of musculoskeletal sarcoma (review). *Oncol Lett*. 2014;8(4):1403–1408.

36. Mohammadi Z, Sazgarnia A, Rajabi O, Soudmand S, Esmaily H, Sadeghi HR. An in vitro study on the photosensitivity of 5-aminolevulinic acid conjugated gold nanoparticles. *Photodiagnosis Photodyn Ther*. 2013;10(4):382–388.

37. Ma X, Qu Q, Zhao Y. Targeted delivery of 5-aminolevulinic acid by multifunctional hollow mesoporous silica nanoparticles for photodynamic skin cancer therapy. *ACS Appl Mater Interfaces*. 2015;7(20):10671–10676.

38. Kars MD, Kara R, Gündoğdu Y, Kepceoğlu A, Kılıç HŞ. Femtosecond laser induced photodynamic therapy on 5-ALA treated SKMEL-30 cells: an efficient theranostic strategy to combat melanoma. *Biomed Pharmacother*. 2014;68(5):657–662.

39. Tetard MC, Vermandel M, Mordon S, Lejeune JP, Reyns N. Experimental use of photodynamic therapy in high grade gliomas: a review focused on 5-aminolevulinic acid. *Photodiagnosis Photodyn Ther*. 2014;11(3):319–330.

40. Colditz MJ, Leyen KV, Jeffree RL. Aminolevulinic acid (ALA)–protoporphyrin IX fluorescence guided tumour resection. Part 2: theoretical, biochemical and practical aspects. *J Clin Neurosci*. 2012;19(12):1611–1616.

41. Stummer W, Pichlmeier U, Meinel T, Wiestler OD, Zanella F. Fluorescence-guided surgery with 5-aminolevulinic acid for resection of malignant glioma: a randomised controlled multicentre phase III trial. *Lancet Oncol*. 2006;7(5):392–401.

42. Ns VDB, van Leeuwen FW, Hg VDP. Fluorescence guidance in urologic surgery. *Curr Opin Urol*. 2012;22(2):109–120.

43. Choi HS, Gibbs SL, Lee JH, et al. Targeted zwitterionic near-infrared fluorophores for improved optical imaging. *Nat Biotechnol*. 2013;31(2):148–153.

44. Zhao X, Zhao H, Chen Z, Zhang D, Lan M. Preparation and characterization of methylene blue-incorporated folate-functionalized Fe_3O_4/mesoporous silica core/shell magnetic nanoparticles. *J Nanosci Nanotechnol*. 2015;15(7):4976–4983.

45. Wirth D, Snuderl M, Curry W, Yaroslavsky A. Comparative evaluation of methylene blue and demeclocycline for enhancing optical contrast of gliomas in optical images. *J Biomed Opt*. 2014; 19(9):90504.

46. van der Vorst JR, Schaafsma BE, Verbeek FP, et al. Intraoperative near-infrared fluorescence imaging of parathyroid adenomas with use of low-dose methylene blue. *Head Neck*. 2014;36(6):853–858.

47. Orloff LA. Methylene blue and sestamibi: complementary tools for localizing parathyroids. *Laryngoscope*. 2001;111(11 pt 1): 1901–1904.

48. Raffaelli M. Systematic review of intravenous methylene blue in parathyroid surgery. *Br J Surg*. 2012;99(10):1345–1352.

49. Schols RM, Connell NJ, Stassen LP. Near-infrared fluorescence imaging for real-time intraoperative anatomical guidance in minimally invasive surgery: a systematic review of the literature. *World J Surg*. 2015;39(5):1069–1079.

50. Nakayama A, Bianco AC, Zhang CY, Lowell BB, Frangioni JV. Quantitation of brown adipose tissue perfusion in transgenic mice using near-infrared fluorescence imaging. *Mol Imaging*. 2003; 2(1):37–49.

51. Tanaka E, Chen FY, Flaumenhaft R, Graham GJ, Laurence RG, Frangioni JV. Real-time assessment of cardiac perfusion, coronary angiography, and acute intravascular thrombi using dual-channel near-infrared fluorescence imaging. *J Thorac Cardiovasc Surg*. 2009;138(1):133–140.

52. Okusanya OT, Madajewski B, Segal E, et al. Small portable interchangeable imager of fluorescence for fluorescence guided surgery and research. *Technol Cancer Res Treat*. 2015;14(2): 213–220.

53. Rey-Dios R, Cohen-Gadol AA. Technical principles and neuro-surgical applications of fluorescein fluorescence using a microscope-integrated fluorescence module. *Acta Neurochir (Wien)*. 2013;155(4):701–706.

54. Mieog JSD, Troyan SL, Hutteman M, et al. Toward optimization of imaging system and lymphatic tracer for near-infrared fluorescent sentinel lymph node mapping in breast cancer. *Ann Surg Oncol*. 2011;18(9):2483–2491.

55. Jafari MD, Wexner SD, Martz JE, et al. Perfusion assessment in laparoscopic left-sided/anterior resection (PILLAR II): a multi-institutional study. *J Am Coll Surg*. 2015;220(1):82–92.e1.

56. Yoshida M, Kubota K, Kuroda J, et al. Indocyanine green injection for detecting sentinel nodes using color fluorescence camera in the laparoscopy-assisted gastrectomy. *J Gastroenterol Hepatol*. 2012;27(suppl 3):29–33.

57. Wada H, Hirohashi K, Anayama T, et al. Minimally invasive electro-magnetic navigational bronchoscopy-integrated near-infrared-guided sentinel lymph node mapping in the porcine lung. *PLoS One*. 2015;10(5):e0126945.

58. Acerbi F, Broggi M, Eoli M, et al. Fluorescein-guided surgery for grade IV gliomas with a dedicated filter on the surgical microscope: preliminary results in 12 cases. *Acta Neurochir (Wien)*. 2013;155(7):1277–1286.

59. Liu Y, Zhao YM, Akers W, et al. First in-human intraoperative imaging of HCC using the fluorescence goggle system and trans-arterial delivery of near-infrared fluorescent imaging agent: a pilot study. *Transl Res*. 2013;162(5):324–331.

60. Liu Y, Bauer AQ, Akers WJ, et al. Hands-free, wireless goggles for near-infrared fluorescence and real-time image-guided surgery. *Surgery*. 2011;149(5):689–698.

61. FullerRuth J. Surgical technology: principles and practice. *Aorn Journal*. 1982;35:1214,6.

62. Keating J, Judy R, Newton A, Singhal S. Near-infrared operating lamp for intraoperative molecular imaging of a mediastinal tumor. *BMC Med Imaging*. 2016;16:15.

63. Wang L, Yu JM, Wang YS, et al. Preoperative lymphoscintigraphy predicts the successful identification but is not necessary in sentinel lymph nodes biopsy in breast cancer. *Ann Surg Oncol*. 2007;14(8):2215–2220.

64. Morton DL, Bostick PJ. Will the true sentinel node please stand?. *Ann Surg Oncol*. 1999;6(1):12–14.

65. Noguchi M, Inokuchi M, Zen Y. Complement of peritumoral and subareolar injection in breast cancer sentinel lymph node biopsy. *J Surg Oncol*. 2009;100(2):100–105.

66. Valdés PA, Leblond F, Jacobs VL, Wilson BC, Paulsen KD, Roberts DW. Quantitative, spectrally-resolved intraoperative fluorescence imaging. *Sci Rep*. 2012;2:798.

67. Stoffels I, Stück HVD, Boy C, et al. Indocyanine green fluorescence-guided sentinel lymph node biopsy in dermato-oncology. *J Dtsch Dermatol Ges*. 2012;10(1):51–57.

68. Buda A, Bussi B, Di MG, et al. Sentinel lymph node mapping with near-infrared fluorescent imaging using Indocyanine green: a new tool for laparoscopic platform in patients with endometrial and cervical cancer. *J Minim Invasive Gynecol*. 2015;23(2):265–269.

69. Vorst JRVD, Schaafsma BE, Verbeek FPR, et al. Randomized comparison of near-infrared fluorescence imaging using indocyanine green and 99m technetium with or without patent blue for the sentinel lymph node procedure in breast cancer patients. *Ann Surg Oncol*. 2012;19(13):4104–4111.

70. Hirche C, Murawa D, Mohr Z, Kneif S, Hünerbein M. ICG fluorescence-guided sentinel node biopsy for axillary nodal staging in breast cancer. *Breast Cancer Res Treat*. 2010;121(2):373–378.

71. Hojo T, Nagao T, Kikuyama M, Akashi S, Kinoshita T. Evaluation of sentinel node biopsy by combined fluorescent and dye method and lymph flow for breast cancer. *Breast*. 2010;19(3):210–213.

72. Murawa D, Hirche C, Dresel S, Hünerbein M. Sentinel lymph node biopsy in breast cancer guided by indocyanine green fluorescence. *Br J Surg*. 2009; 96(11):1289–1294.

73. Tagaya N, Yamazaki R, Nakagawa A, et al. Intraoperative identification of sentinel lymph nodes by near-infrared fluorescence imaging in patients with breast cancer. *Am J Surg*. 2008;195(6):850–853.

74. Guo W, Zhang L, Ji J, Gao W, Liu J, Tong M. Breast cancer sentinel lymph node mapping using near-infrared guided indocyanine green in comparison with blue dye. *Tumour Biol*. 2014;35(4):3073–3078.

75. Hirche C, Mohr Z, Kneif S, et al. Ultrastaging of colon cancer by sentinel node biopsy using fluorescence navigation with indocyanine green. *Int J Colorectal Dis*. 2012;27(3):319–324.

76. Cahill RA, Bembenek A, Sirop S, et al. Sentinel node biopsy for the individualization of surgical strategy for cure of early-stage colon cancer. *Ann Surg Oncol*. 2009;16(8):2170–2180.

77. Park JS, Chang IT, Park SJ, et al. Comparison of ex vivo and in vivo injection of blue dye in sentinel lymph node mapping for colorectal cancer. *World J Surg*. 2009;33(3):539–546.

78. Hutteman M, Choi HS, Mieog JS, et al. Clinical translation of ex vivo sentinel lymph node mapping for colorectal cancer using invisible near-infrared fluorescence light. *Ann Surg Oncol*. 2010;18(4):1006–1014.

79. Liberale G, Vankerckhove S, Galdon MG, Donckier V, Larsimont D, Bourgeois P. Fluorescence imaging after intraoperative intravenous injection of indocyanine green for detection of lymph node metastases in colorectal cancer. *Eur J Surg Oncol*. 2015; 41(9):1256–1260.

80. Miyashiro I, Kishi K, Yano M, et al. Laparoscopic detection of sentinel node in gastric cancer surgery by indocyanine green fluorescence imaging. *Surg Endosc*. 2011;25(5):1672–1676.

81. Herrera-Almario G, Patane M, Sarkaria I, Strong VE. Initial report of near-infrared fluorescence imaging as an intraoperative adjunct for lymph node harvesting during robot-assisted laparoscopic gastrectomy. *J Surg Oncol*. 2016;113(7):768–770.

82. Adams S, Baum RP, Hertel A, et al. Intraoperative gamma probe detection of neuroendocrine tumors. *J Nucl Med*. 1998;39(7):1155–1160.

83. Keating J, Tchou J, Okusanya O, et al. Identification of breast cancer margins using intraoperative near-infrared imaging. *J Surg Oncol*. 2016;113(5):508–514.

84. Keereweer S, Kerrebijn JD, van Driel PB, et al. Optical image-guided surgery—where do we stand? *Mol Imaging Biol*. 2011; 13(2):199–207.

85. Sevick-Muraca EM. Translation of near-infrared fluorescence imaging technologies: emerging clinical applications. *Annu Rev Med*. 2012;63:217–231.

86. Kleinjan GH, Brouwer OR, Mathéron HM, et al. Hybrid radioguided occult lesion localization (hybrid ROLL) of (18)F-FDG-avid lesions using the hybrid tracer indocyanine green-(99m)Tc-nanocolloid. *Rev Esp Med Nucl Imagen Mol*. 2016;35(5):292–297.

87. Ishizawa T, Fukushima N, Shibahara J, et al. Real-time identification of liver cancers by using indocyanine green fluorescent imaging. *Cancer*. 2009;115(11):2491–2504.

88. Yokoyama N, Otani T, Hashidate H, et al. Real-time detection of hepatic micrometastases from pancreatic cancer by intraoperative fluorescence imaging. *Cancer*. 2012;118(11):2813–2819.

89. Iida G, Asano K, Seki M, et al. Intraoperative identification of canine hepatocellular carcinoma with indocyanine green fluorescent imaging. *J Small Anim Pract*. 2013;54(11):594–600.

90. Satou S, Ishizawa T, Masuda K, et al. Indocyanine green fluorescent imaging for detecting extrahepatic metastasis of hepatocellular carcinoma. *J Gastroenterol*. 2013;48(10):1136–1143.

91. Abo T, Nanashima A, Tobinaga S, et al. Usefulness of intraoperative diagnosis of hepatic tumors located at the liver surface and hepatic segmental visualization using indocyanine green-photodynamic eye imaging. *Eur J Surg Oncol*. 2015;41(2):257–264.

92. Zeng C, Shang W, Wang K, et al. Intraoperative identification of liver cancer microfoci using a targeted near-infrared fluorescent probe for imaging-guided surgery. *Sci Rep*. 2016;6:21959.

93. Della PA, Rustemi O, Gioffrè G, et al. Predictive value of intraoperative 5-aminolevulinic acid-induced fluorescence for detecting bone invasion in meningioma surgery. *J Neurosurg*. 2014;120(4):840–845.

94. Millesi M, Kiesel B, Woehrer A, et al. Analysis of 5-aminolevulinic acid-induced fluorescence in 55 different spinal tumors. *Neurosurg Focus*. 2014;36(2):E11.

95. Valle RD, Solis ST, Gastearena MAI, Eulate RGD, Echávarri PD, Mendiroz JA. Surgery guided by 5-aminolevulinic fluorescence in glioblastoma: volumetric analysis of extent of resection in single-center experience. *J Neurooncol*. 2011;102(1):105–113.

96. Roberts DW, Valdés PA, Harris BT, et al. Coregistered fluorescence-enhanced tumor resection of malignant glioma: relationships between δ-aminolevulinic acid-induced protoporphyrin IX fluorescence, magnetic resonance imaging enhancement, and neuropathological parameters. Clinical article. *J Neurosurg*. 2011;114(3):595–603.

97. Hefti M, Von CG, Moschopulos M, Siegner A, Looser H, Landolt H. 5-aminolevulinic acid induced protoporphyrin IX fluorescence in high-grade glioma surgery: a one-year experience at a single institutuion. *Swiss Med Wkly*. 2008;138(11-12):180–185.

98. Stummer W, Tonn JC, Goetz C, et al. 5-Aminolevulinic acid-derived tumor fluorescence: the diagnostic accuracy of visible fluorescence qualities as corroborated by spectrometry and histology and postoperative imaging. *Neurosurgery*. 2014;74(3):310–320.

99. Lau D, Hervey-Jumper SL, Chang S, et al. A prospective phase II clinical trial of 5-aminolevulinic acid to assess the correlation of intraoperative fluorescence intensity and degree of histologic cellularity during resection of high-grade gliomas. *J Neurosurg*. 2015;124(5):1300–1309.

100. Valdés PA, Kim A, Brantsch M, et al. δ-Aminolevulinic acid-induced protoporphyrin IX concentration correlates with histopathologic markers of malignancy in human gliomas: the need for quantitative fluorescence-guided resection to identify regions of increasing malignancy. *Neuro Oncol*. 2011;13(8):846–856.

101. Schucht P, Beck J, Abu-Isa J, et al. Gross total resection rates in contemporary glioblastoma surgery: results of an institutional protocol combining 5-aminolevulinic acid intraoperative fluorescence imaging and brain mapping. *Neurosurgery*. 2012;71(5):927–935; discussion 935-936.

102. Coburger J, Hagel V, Wirtz CR, König R. Surgery for glioblastoma: impact of the combined use of 5-aminolevulinic acid and intraoperative MRI on extent of resection and survival. *PLoS One*. 2015;10(6):e0131872.

103. Tsugu A, Ishizaka H, Mizokami Y, et al. Impact of the combination of 5-aminolevulinic acid-induced fluorescence with intraoperative magnetic resonance imaging-guided surgery for glioma. *World Neurosurg*. 2011;76(1-2):120–127.

104. Arita H, Kinoshita M, Kagawa N, et al. ^{11}C-methionine uptake and intraoperative 5-aminolevulinic acid-induced fluorescence as separate index markers of cell density in glioma. *Cancer*. 2012;118(6):1619–1627.

105. Orringer DA, Koo YE, Chen T, et al. In vitro characterization of a targeted, dye-loaded nanodevice for intraoperative tumor delineation. *Neurosurgery*. 2009;64(5):965–971; discussion 971-972.

106. Akopov A, Rusanov A, Gerasin A, Kazakov N, Urtenova M, Chistyakov I. Preoperarive endobronchial photodinamic therapy improves resectability in initially irresectable (inoperable) locally advanced non small cell lung cancer. *Photodiagnosis Photodyn Ther*. 2014;11(3):259–264.

107. Muragaki Y, Akimoto J, Maruyama T, et al. Phase II clinical study on intraoperative photodynamic therapy with talaporfin sodium and semiconductor laser in patients with malignant brain tumors. *J Neurosurg*. 2013;119(4):845–852.

108. Poorten VV, Meulemans J, Nuyts S, et al. Postoperative photodynamic therapy as a new adjuvant treatment after robot-assisted salvage surgery of recurrent squamous cell carcinoma of the base of tongue. *World J Surg Oncol*. 2015;13(1):214.

109. Stylli SS, Kaye AH, Macgregor L, Howes M, Rajendra P. Photodynamic therapy of high grade glioma—long term survival. *J Clin Neurosci*. 2005;12(4):389–398.

110. Eljamel MS, Goodman C, Moseley H. ALA and Photofrin® fluorescence-guided resection and repetitive PDT in glioblastoma multiforme: a single centre phase III randomised controlled trial. *Lasers Med Sci*. 2008;23(4):361–367.

111. Xiao H, Liao Q, Cheng M, et al. 5-Amino-4-oxopentanoic acid photodynamic diagnosis guided microsurgery and photodynamic therapy on VX2 brain tumour implanted in a rabbit model. *Chin Med J (Engl)*. 2009;122(11):1316–1321.

112. Stepp HG, Beck T, Beyer W, Sroka R. Fluorescence-guided resections and photodynamic therapy for malignant gliomas using 5-aminolevulinic acid. *Proc SPIE Int Soc Opt Eng*. 2005;5686:547–557.

113. Choi Y, Kim S, Choi MH, et al. Photodynamic therapy: highly biocompatible carbon nanodots for simultaneous bioimaging and targeted photodynamic therapy in vitro and in vivo. *Adv Funct Mater*. 2014;24(37):5774.

114. Wang C, Cheng L, Liu Y, et al. Biomedical applications: imaging-guided ph-sensitive photodynamic therapy using charge reversible upconversion nanoparticles under near-infrared light. *Adv Funct Mater*. 2013;23(24):3077–3086.

115. Song X, Liang C, Gong H, Chen Q, Wang C, Liu Z. Photosensitizer-conjugated albumin–polypyrrole nanoparticles for imaging-guided in vivo photodynamic/photothermal therapy. *Small*. 2015;11(32):3932–3941.

116. Taratula O, Patel M, Schumann C, et al. Phthalocyanine-loaded graphene nanoplatform for imaging-guided combinatorial phototherapy. *Int J Nanomedicine*. 2015;10:2347–2362.

117. Rong P, Yang K, Srivastan A, et al. Photosensitizer loaded nano-graphene for multimodality imaging guided tumor photodynamic therapy. *Theranostics*. 2014;4(3):229–239.

118. Srivatsan A, Jenkins SV, Jeon M, et al. Gold nanocage-photosensitizer conjugates for dual-modal image-guided enhanced photodynamic therapy. *Theranostics*. 2014;4(2):163–174.

119. Ai J, Xu Y, Lou B, Li D, Wang E. Multifunctional AS1411-functionalized fluorescent gold nanoparticles for targeted cancer cell imaging and efficient photodynamic therapy. *Talanta*. 2014;118:54–60.

120. Panchenko PA, Sergeeva AN, Fedorova OA, et al. Spectroscopical study of bacteriopurpurinimide-naphthalimide conjugates for fluorescent diagnostics and photodynamic therapy. *J Photochem Photobiol B*. 2014;133:140–144.

121. Huang P, Lin J, Wang S, et al. Photosensitizer-conjugated silica-coated gold nanoclusters for fluorescence imaging-guided photodynamic therapy. *Biomaterials*. 2013;34(19):4643–4654.

122. Koo H, Lee H, Lee S, et al. In vivo tumor diagnosis and photodynamic therapy via tumoral pH-responsive polymeric micelles. *Chem Commun (Camb)*. 2010;46(31):5668–5670.

123. Lovell JF, Jin CS, Huynh E, MacDonald TD, Cao W, Zheng G. Enzymatic regioselection for the synthesis and biodegradation of porphysome nanovesicles. *Angew Chem Int Ed Engl*. 2012;51(10):2429–2433.

124. Du J, O'Reilly RK. Anisotropic particles with patchy, multicompartment and Janus architectures: preparation and application. *Chem Soc Rev*. 2011;40(5):2402–2416.

125. Yi X, Wang F, Qin W, Yang X, Yuan J. Near-infrared fluorescent probes in cancer imaging and therapy: an emerging field. *Int J Nanomedicine*. 2014;9:1347–1365.

126. Abouelmagd SA, Hyun H, Yeo Y. Extracellularly activatable nanocarriers for drug delivery to tumors. *Expert Opin Drug Deliv*. 2014;11(10):1601–1618.

127. Hu JJ, Liu LH, Li ZY, Zhuo RX, Zhang XZ. MMP-responsive theranostic nanoplatform based on mesoporous silica nanoparticles for tumor imaging and targeted drug delivery. *J Mater Chem B Mater Biol Med*. 2016;4(11):1932–1940.

128. Kim J, Tung CH, Choi Y. Smart dual-functional warhead for folate receptor-specific activatable imaging and photodynamic therapy. *Chem Commun (Camb)*. 2014;50(73):10600–10603.

129. Schneider R, Schmitt F, Frochot C, et al. Design, synthesis, and biological evaluation of folic acid targeted tetraphenylporphyrin as novel photosensitizers for selective photodynamic therapy. *Bioorg Med Chem*. 2005;13(8):2799–2808.

130. Wang F, Chen X, Zhao Z, et al. Synthesis of magnetic, fluorescent and mesoporous core-shell-structured nanoparticles for imaging, targeting and photodynamic therapy. *J Mater Chem*. 2011;21(30):11244–11252.

131. Zhang C, Li C, Liu Y, et al. Gold nanoclusters-based nanoprobes for simultaneous fluorescence imaging and targeted photodynamic therapy with superior penetration and retention behavior in tumors. *Adv Funct Mater*. 2015;25(8):1314–1325.

132. Soundararajan S, Chen W, Spicer EK, Courtenayluck N, Fernandes DJ. The nucleolin targeting aptamer AS1411 destabilizes Bcl-2 messenger RNA in human breast cancer cells. *Cancer Res*. 2008;68(7):2358–2365.

133. Laabs E, Béhé M, Kossatz S, Frank W, Kaiser WA, Hilger I. Optical imaging of CCK$_2$/gastrin receptor-positive tumors with a minigastrin near-infrared probe. *Invest Radiol*. 2011;46(3):196–201.

134. Rizvi SB, Rouhi S, Taniguchi S, et al. Near-infrared quantum dots for HER2 localization and imaging of cancer cells. *Int J Nanomedicine*. 2014;9:1323–1337.

135. Yoon HY, Koo H, Choi KY, et al. Tumor-targeting hyaluronic acid nanoparticles for photodynamic imaging and therapy. *Biomaterials*. 2012;33(15):3980–3989.

136. Lv PC, Roy J, Putt KS, Low PS. Evaluation of a carbonic anhydrase IX-targeted near-infrared dye for fluorescence-guided surgery of hypoxic tumors. *Mol Pharm*. 2016;13(5):1618–1625.